Biphasic functions for the GDNF-Ret signaling pathway in chemosensory neuron development and diversification

Christopher R. Donnelly[a], Amol A. Shah[a], Charlotte M. Mistretta[a], Robert M. Bradley[a], and Brian A. Pierchala[a,1]

[a]Department of Biologic and Materials Sciences, University of Michigan, Ann Arbor, MI 48109

Edited by Solomon H. Snyder, Johns Hopkins University School of Medicine, Baltimore, MD, and approved November 21, 2017 (received for review May 27, 2017)

The development of the taste system relies on the coordinated regulation of cues that direct the simultaneous development of both peripheral taste organs and innervating sensory ganglia, but the underlying mechanisms remain poorly understood. In this study, we describe a novel, biphasic function for glial cell line-derived neurotrophic factor (GDNF) in the development and subsequent diversification of chemosensory neurons within the geniculate ganglion (GG). GDNF, acting through the receptor tyrosine kinase Ret, regulates the expression of the chemosensory fate determinant Phox2b early in GG development. *Ret*$^{-/-}$ mice, but not *Ret*$^{fx/fx}$; *Phox2b*-Cre mice, display a profound loss of Phox2b expression with subsequent chemosensory innervation deficits, indicating that Ret is required for the initial amplification of Phox2b expression but not its maintenance. Ret expression is extinguished perinatally but reemerges postnatally in a subpopulation of large-diameter GG neurons expressing the mechanoreceptor marker NF200 and the GDNF coreceptor GFRα1. Intriguingly, we observed that ablation of these neurons in adult *Ret*-Cre/ER^{T2}; *Rosa26*$^{LSL\text{-}DTA}$ mice caused a specific loss of tactile, but not chemical or thermal, electrophysiological responses. Overall, the GDNF-Ret pathway exerts two critical and distinct functions in the peripheral taste system: embryonic chemosensory cell fate determination and the specification of lingual mechanoreceptors.

Ret | taste | Phox2b | chemosensory | geniculate

Creating the neuronal diversity required to appropriately discriminate different kinds of sensory stimuli, including all aspects of somatosensory, taste, visual, auditory, and olfactory stimuli, is a complex task during vertebrate development. Following neurogenesis, one means of differentiating and specifying unique sensory neuron subpopulations is by selective expression of transcription factors and neurotrophic factor receptors (1). These signaling pathways regulate the expression of additional transcription factors, ion channels, neurotransmitter receptors, and neuropeptides that define the molecular and functional characteristics of different classes of sensory neurons (2). The selective expression of distinct neurotrophic factor receptors is one potential means of delineating functionally distinct populations of somatosensory neurons within the dorsal root ganglion (DRG) and trigeminal ganglion (TG). For example, while TrkB+ large-diameter mechanoreceptive neurons afferently innervate Merkel cells and lanceolate endings producing BDNF (3), TrkA+ small- and medium-diameter neurons mediating pain sensation project free nerve endings to the skin where NGF is produced (4). Because heterogeneous sensory neurons responsive to temperature, touch, and all five taste qualities cohabitate within the peripheral taste ganglia (5–7), this system is well-suited to exploring the underlying molecular mechanisms regulating sensory neuron diversification and physiology. The geniculate ganglion (GG) houses soma for taste and thermal afferents to lingual taste buds (TBs) in the fungiform papillae, projecting via the chorda tympani (CT) nerve. Although a major taste ganglion for the anterior tongue, the GG also includes neurons innervating TBs on the soft palate as well as somatosensory neurons projecting to the external ear (8). This major ganglion for orofacial sensation is complex and multimodal, with soma for taste, touch, and lingual temperature reception (5–7). However, our knowledge of the molecular mechanisms dictating GG chemosensory neuron development and postnatal heterogeneity remain poorly understood, especially compared with primary sensory afferent neurons in the DRG and TG.

Previous studies have focused on the role of the neurotrophins in chemosensory GG development and maintenance, with NT-4 and BDNF emerging as the principal regulators of GG axon guidance (9), GG neuron survival (10), and CT nerve regeneration (11). Despite these advances in our understanding of the development and postnatal maintenance of the peripheral taste system, our knowledge of the roles of other inductive cues involved in sensory neuron specification and diversity remains rudimentary. Additionally, although there is some evidence supporting the presence of molecularly and functionally distinct subpopulations of GG neurons, our knowledge as to the signaling pathways or markers that shape the multimodal nature of GG neurons is lacking.

Another family of neurotrophic factors, the glial cell line-derived neurotrophic factor (GDNF) family ligands (GFLs), consisting of GDNF, neurturin, artemin, and persephin, contains four

Significance

While knowledge of signaling mechanisms orchestrating the development and diversification of peripheral somatosensory neurons is extensive, our understanding of the mechanisms controlling chemosensory neuron specification remains rudimentary. Lingually projecting sensory neurons of the geniculate ganglion are receptive to the five taste qualities, as well as temperature and tactile stimuli, but the mechanisms responsible for the diversification of the unique subpopulations that respond to one, or several, of these stimuli remain unknown. Here we demonstrate that the GDNF-Ret signaling pathway exerts a unique, dual function in peripheral taste system development and postnatal function. Ret acts embryonically to regulate the expression of the chemosensory master regulator Phox2b, thus inducing chemosensory differentiation, while postnatally acting to specify a molecularly unique subpopulation of lingual mechanoreceptors.

Author contributions: C.R.D., C.M.M., and B.A.P. designed research; C.R.D., A.A.S., and R.M.B. performed research; C.R.D. contributed new reagents/analytic tools; C.R.D., A.A.S., C.M.M., R.M.B., and B.A.P. analyzed data; and C.R.D., A.A.S., C.M.M., R.M.B., and B.A.P. wrote the paper.

The authors declare no conflict of interest.

This article is a PNAS Direct Submission.

[1]To whom correspondence should be addressed. Email: pierchal@umich.edu.

This article contains supporting information online at www.pnas.org/lookup/suppl/doi:10.1073/pnas.1708838115/-/DCSupplemental.

homologous growth factors critical for the development of several populations of peripheral neurons, including autonomic neurons (12), rapidly adapting mechanoreceptors (13), and nonpeptidergic nociceptor populations (14) within the DRG sensory system. The receptor tyrosine kinase Ret conveys the trophic functions of the GFLs (15). Importantly, Ret is highly expressed in the GG early in embryonic development (16), and stimulation of early embryonic GG neurons with GDNF promotes axon outgrowth (17), indicating that the GDNF receptor components are present and poised to exert trophic effects in developing GG sensory neurons.

In this study, we investigated the function of the GDNF-Ret signaling pathway in the development and subsequent postnatal diversification of chemosensory neurons within the GG. To discern the developmental requirement, as well as the molecular and neurophysiological signatures for GG cells and GG/CT afferents, we have used expression analyses, genetic models, pharmacologic inhibitors, and neurophysiological approaches. Collectively, we identify a novel, biphasic function for GDNF-Ret signaling in the peripheral taste system, initially acting to promote the chemosensory phenotype of all GG neurons, while acting postnatally to define a unique subpopulation of lingual mechanoreceptors. These data significantly broaden our understanding of the cues responsible for taste neuron development, and bring to light new concepts for understanding GG biology and peripheral sensory circuits of the tongue.

Results

Ret Is Widely Expressed by Geniculate Chemosensory Neurons at E13.5, but Expression Is Extinguished Perinatally. A previous study describing the transcriptional profile of GG neurons indicated that a combinatorial expression pattern of Tlx3$^+$/Islet$^+$/Phox2b$^+$/Phox2a$^+$/Brn3a$^-$ coincides with a chemosensory neuronal fate, while a Tlx3$^+$/Islet$^+$/Phox2b$^-$/Phox2a$^-$/Brn3a$^+$ transcriptional code coincides with a somatosensory fate. In this study, Phox2b was discovered to serve in sensory neurons as a master regulator commanding a visceral, chemosensory fate, while repressing a somatosensory fate (16). In this way, the geniculate ganglion exerts a strong polarity between the distal chemosensory neurons innervating the anterior two-thirds of the tongue and the proximal somatosensory neurons innervating the external ear. Curiously, upon qualitative analysis using in situ hybridization, the authors also found strong Ret expression which was correlated with a Phox2b$^+$/Brn3a$^-$ chemosensory transcriptional profile as early as E11.5 (16). Importantly, these data suggest that Ret is one of the earliest growth factor receptors expressed by GG neurons, and may be selectively functioning within chemosensory neurons. We quantified the proportion of chemosensory and somatosensory neurons expressing Ret during embryonic development of the GG. For these purposes, chemosensory neurons were defined as TuJ1+ neurons expressing Phox2b, while somatosensory neurons were those lacking Phox2b expression. To validate the use of Phox2b as a specific marker of chemosensory neurons (18), we conducted immunolabeling of Phox2b, RFP (which detects the tdTomato protein), and TuJ1 (a pan-neuronal marker) in GG and TG from postnatal day (P)0 *Rosa26*$^{LSL\text{-}TdTomato/+}$; *Phox2b-Cre*$^{tg/+}$ mice. TGs, known to be Phox2b$^-$/Brn3a$^+$, were analyzed as a negative control (19). For the specificity of RFP immunolabeling, *Rosa26*$^{LSL\text{-}TdTomato/+}$; *Phox2b-Cre*$^{+/+}$ mice were also analyzed. We observed that 98.84% of neurons reactive for Phox2b immunostaining were also RFP+, indicating a high reliability of this Phox2b antibody in labeling chemosensory neurons (98.84 ± 0.11%; Fig. S1*A*). Further validating the use of Phox2b as a marker of chemosensory neurons, we found that 0.03% of TG neurons exhibited labeling for Phox2b and, in all cases, these neurons were RFP+ (Fig. S1*B*). The majority of RFP+ immunolabeling in the TG was restricted to axons, likely due to labeling of trigeminal motor axons passing through the ganglion. These data confirm the high fidelity of Phox2b immunolabeling of chemosensory neurons and validate the use of the *Phox2b-Cre*$^{tg/+}$ line.

To determine the spatiotemporal expression pattern of Ret in the GG, we performed a tamoxifen (TMX) pulse-labeling experiment using a Cre-inducible tomato reporter line (*Rosa26*$^{LSL\text{-}TdTomato}$) crossed to Ret-Cre/ER^{T2} mice (13). Importantly, we used this reporter strategy to avoid limitations in specificity observed with Ret immunostaining. Two time periods were analyzed (outlined in Fig. 1*A*): four daily TMX injections from E9.5 to E12.5, with analysis performed at E13.5; or four daily TMX injections from E14.5 to E17.5, with analysis conducted at E18.5. Notably, analysis of these early and late embryonic time points allowed an examination into Ret expression during periods corresponding to transcriptional diversification and target innervation, respectively (8, 20). Ganglia were immunolabeled for TuJ1, Phox2b, and RFP, and total numbers of chemosensory (Fig. 1*B*) and somatosensory (Fig. 1*C*) neurons expressing Ret were quantified. Coinciding with previous studies, we found that the majority of chemosensory neurons were Ret+ at E13.5 (69.41 ± 4.35%) but expression was greatly reduced by E18.5 (3.38 ± 0.42%) (Fig. 1 *B–F*). Additionally, very few somatosensory neurons expressed Ret at either time point analyzed (Fig. 1 *B–F*).

Given that Ret is highly expressed by chemosensory GG neurons before lingual innervation, we hypothesized that the Ret ligand GDNF is present locally, acting on Ret+ chemosensory neurons. To test this hypothesis, we used a TMX pulse-labeling experiment using *Rosa26*$^{LSL\text{-}TdTomato}$; *GDNF*-IRES-Cre/ER^{T2} (*GDNF*$^{Cre/+}$) mice (21) and analyzed the previously described time points (Fig. 1*A*). Heads were collected from E13.5 and E18.5 labeled mice and immunolabeling was again performed for TuJ1, Phox2b, and RFP (to label GDNF+ cells). Surprisingly, GDNF expression was restricted to GG neurons themselves, rather than the surrounding tissues (Fig. S2). Similar to the Ret expression quantifications, we observed that many chemosensory neurons express GDNF at E13.5 (27.14 ± 0.85%) but expression is virtually lost by E18.5 (4.31 ± 0.22%) (Fig. S2 *A* and *C*). Additionally, few somatosensory neurons express GDNF at E13.5 (0.43 ± 0.06%) or E18.5 (8.62 ± 1.45%) (Fig. S2 *B* and *C*). Collectively, these data suggest that a GDNF-Ret paracrine signaling pathway exists in chemosensory GG neurons early in development.

Ret Is Required for Expression of the Chemosensory Fate Determinant Phox2b but Not Brn3a or TrkB. Sensory neuron diversification relies on differential transcriptional activities that induce and maintain expression of required growth factor receptors, and these receptors in turn serve activator or repressor functions (2). The expression of Ret within the E9.5-to-E12.5 developmental window, but not within E14.5 to E17.5, suggests an early role in chemosensory fate determination. It is during this embryonic period that GG neurons begin their initial transcriptional fate acquisition (16) and initial axon outgrowth, but they do not reach their final targets until at least 1 d later (8). Given this timeline, we hypothesized that Ret is unlikely to be involved in target innervation but rather may play a role in early transcriptional diversification. Therefore, we analyzed total GG neuron numbers and the proportion of Phox2b+ neurons in *Ret*$^{-/-}$ mice (22) (or *Ret*$^{+/+}$ mice, as a control) (Fig. 2 *A–C*). Strikingly, although no difference was observed in the total number of neurons (*Ret*$^{+/+}$: 767.63 ± 29.35 neurons vs. *Ret*$^{-/-}$: 761.35 ± 35.33 neurons; P = 0.9014; Fig. 2 *A* and *B*), we observed a significant reduction in the proportion of neurons with detectable Phox2b immunolabeling (*Ret*$^{+/+}$: 73.78 ± 2.17% vs. *Ret*$^{-/-}$: 44.00 ± 5.84%; 40.4% reduction; P = 0.0015). There was also a substantially reduced intensity of Phox2b in neurons that retained a positive signal (Fig. 2*D*). To determine whether this loss of Phox2b expression was coupled with a change in the proportion of neurons expressing the somatosensory transcriptional fate determinant Brn3a (23) or the

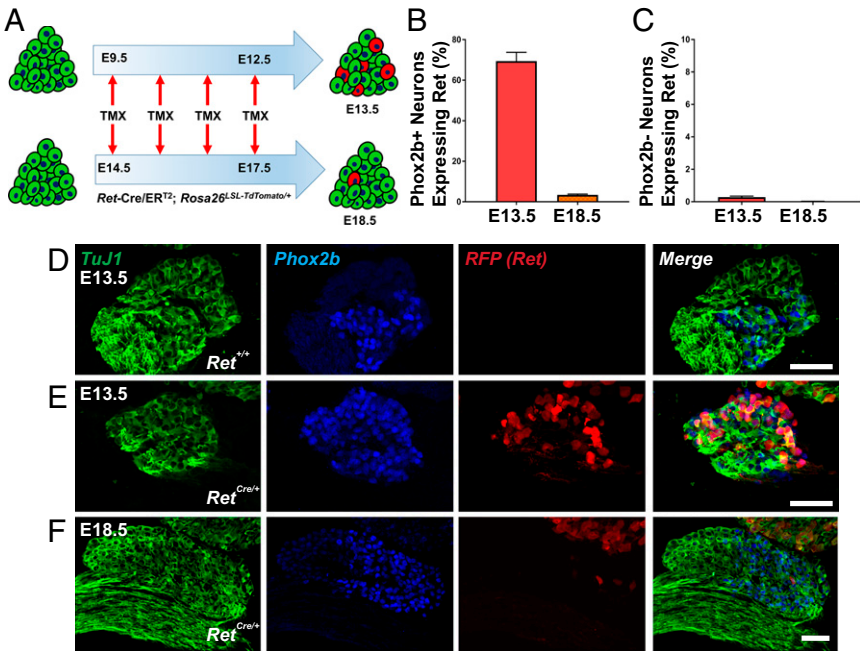

Fig. 1. Ret is highly expressed in chemosensory geniculate neurons early in development. (*A*) Experimental strategy for tracing Ret expression in embryonic geniculate ganglia. Tamoxifen was administered to Ret-Cre/ER^{T2}; *Rosa26*$^{LSL\text{-}TdTomato/+}$ reporter mice at E9.5 to E12.5 with E13.5 analysis (*Upper*) and E14.5 to E17.5 with E18.5 analysis (*Lower*). (*B*) Quantification of the proportion of chemosensory (Phox2b+) neurons expressing Ret demonstrates widespread expression within chemosensory neurons (E13.5; $n = 3$), but Ret expression is extinguished perinatally (E18.5; $n = 4$). (*C*) Quantification of the proportion of somatosensory (Phox2b–) neurons expressing Ret. (*D–F*) Immunofluorescence with TuJ1 (green), Phox2b (blue), and RFP (indicating Ret; red) with merged images (*Right*). (*D*) Staining in a *Ret*$^{+/+}$ littermate demonstrates the specificity of the RFP antibody. (*E* and *F*) Ret was widely expressed in chemosensory neurons at the E13.5 analysis time point (*E*) but largely absent upon analysis at E18.5 (*F*). Note that the TG in the upper right hand corner of *F* has many Ret+ neurons at E18.5. Error bars indicate mean ± SEM. (Scale bars, 50 μm.)

broadly expressed TrkB receptor involved in GG survival (24), we examined TuJ1, Brn3a, and TrkB expression, followed by quantification of the proportion of each subgroup. There was no change in the proportion of neurons expressing Brn3a (*Ret*$^{+/+}$: 32.67 ± 2.37% vs. *Ret*$^{-/-}$: 30.60 ± 6.57%; $P = 0.7587$; Fig. 2 *F* and *G*). Likewise, there was no change in the proportion of neurons expressing TrkB (Fig. 2 *E* and *G*), which was expressed widely in both chemosensory and somatosensory GG neurons alike (*Ret*$^{+/+}$: 97.06 ± 0.49% vs. *Ret*$^{-/-}$: 98.08 ± 0.31%; $P = 0.1161$). To validate our immunostaining for TrkB, we also immunostained for TuJ1, Islet1 (a pan-sensory neuron marker), and GFP on P0 TGs isolated from *TrkB*$^{GFP/+}$ or *TrkB*$^{GFP/GFP}$ mice. TrkB labeling overlapped nearly completely with GFP in *TrkB*$^{GFP/+}$ mice, which retain one functional copy of TrkB protein, but no TrkB immunolabeling was observed in *TrkB*$^{GFP/GFP}$ knockout mice (3), despite the presence of GFP+ neurons (Fig. S3).

Ret Is Required for the Amplification of Phox2b. Two possibilities can explain the loss of Phox2b expression in Ret knockout mice at E18.5: (*i*) Ret is required for the initiation of Phox2b expression within the chemosensory GG population; or (*ii*) Ret is required for the amplification of Phox2b expression within chemosensory GG neurons. To distinguish between these two, we crossed Ret conditional knockout mice (*Ret*$^{fx/fx}$) (14) with *Phox2b*-Cre$^{tg/+}$ mice (Ret-cKO). *Ret*$^{fx/fx}$; *Phox2b*-Cre$^{+/+}$ (Ret-WT) mice were analyzed as a control. These mice will only undergo recombination following initiation of Phox2b expression, thereby testing whether Ret is needed for the initiation of Phox2b. Tissues were immunostained for Phox2b and TuJ1, and total neuron numbers and the proportion of Phox2b+ GG neurons were quantified. Interestingly, there was no difference in total neuron numbers (Fig. S4 *A* and *B*; Ret-WT: 723.60 ± 13.47 vs. Ret-cKO: 789.15 ± 25.43; $P = 0.0712$) or in the proportion of Phox2b+ neurons (Fig. S4; Ret-WT: 65.07 ± 1.02% vs. Ret-cKO: 61.39 ± 2.98%; $P = 0.3503$), indicating that Ret is dispensable for Phox2b maintenance. To further explore this hypothesis, we crossed Ret conditional knockout mice with conventional germ-line knockout mice to generate *Ret*$^{fx/-}$ mice (and *Ret*$^{fx/+}$ mice as a control). The Ret conditional knockout mice were created to harbor a single-nucleotide missense mutation (V805A) in the kinase domain, which is functionally silent but makes Ret in these mice susceptible to a highly selective chemical inhibition of kinase activity with the pharmacologic inhibitor 1NM-PP1 (25). Ret signaling generally functions via a positive feedback loop, where Ret activation promotes further Ret expression and blocking Ret activation therefore impairs Ret expression (14, 26). We used this system as a reversible means of reducing Ret levels and activity during a defined developmental time window.

To verify that daily systemic administration of 1NM-PP1 was effective in reducing total Ret levels, pregnant dams were injected daily with 1NM-PP1 from E14.5 to E17.5 and spinal cords were isolated from E18.5 *Ret*$^{fx/+}$ and *Ret*$^{fx-}$ embryos, followed by quantitative immunoblotting for Ret and actin (as a loading control; Fig. 3*A*). This is an especially strict confirmation of Ret knockdown, as 1NM-PP1 must pass through the blood–brain barrier to achieve adequate inhibition of spinal cord neurons, in contrast to the GG in the periphery. Importantly, we observed that administration of 1NM-PP1 to *Ret*$^{fx/-}$ mice led to a substantial reduction in total Ret levels, as predicted [*Ret*$^{fx/+}$: 1.00 ± 0.19 arbitrary units (a.u.) vs. 0.23 ± 0.05 a.u.; 77% reduction; $P = 0.0048$; Fig. 3*B*]. Having demonstrated that this technique is effective in knocking down Ret in a temporally controlled manner, we administered 1NM-PP1 to *Ret*$^{fx/-}$ and *Ret*$^{fx/+}$ mice from E9.5 to E12.5, with analysis at E18.5, and from E13.5 to E17.5, with analysis at E18.5. Interestingly, compared with GGs collected from *Ret*$^{fx/+}$ mice, *Ret*$^{fx/-}$ animals administered 1NM-PP1

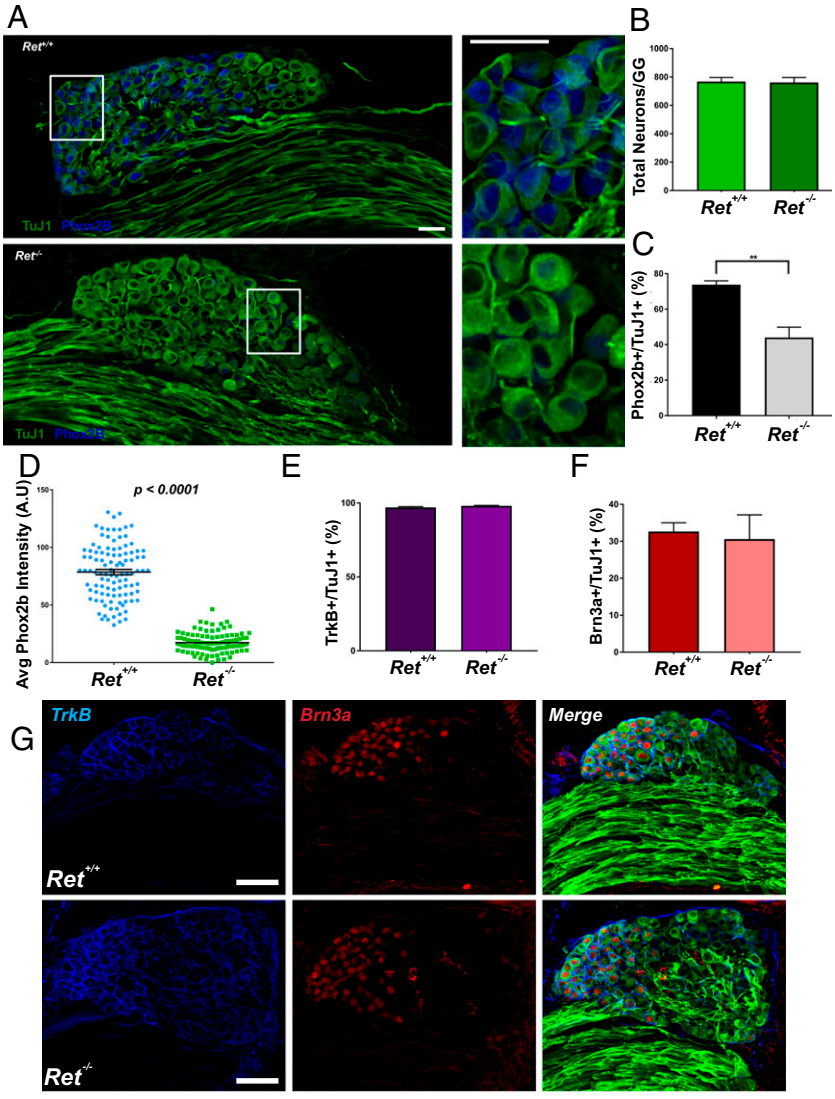

Fig. 2. Ret is required for the expression of the chemosensory fate determinant Phox2b but is dispensable for chemosensory neuron survival. (*A*) GGs were taken from E18.5 $Ret^{+/+}$ and $Ret^{-/-}$ mice and immunostained for TuJ1 and Phox2b. (*A*, *Left*) Entire ganglion. (*A*, *Right*) Magnification of the areas bordered by the white boxes. $Ret^{-/-}$ mice had substantially fewer Phox2b+ neurons, and those with residual expression appeared reduced in Phox2b staining intensity. (*B*) The total number of GG neurons was assessed by counting TuJ1+ neurons. No difference was observed in total numbers of $Ret^{+/+}$ GGs ($n = 6$) compared with $Ret^{-/-}$ GGs ($n = 9$) ($P = 0.9014$). (*C*) Quantification of the proportion of neurons expressing Phox2b. $Ret^{-/-}$ GGs had a reduction in Phox2b+ neurons compared with $Ret^{+/+}$ GGs (40.1% reduction; $P = 0.0015$). (*D*) The intensity of Phox2b expression was quantified in $Ret^{+/+}$ and $Ret^{-/-}$ GGs. $Ret^{-/-}$ GGs had significantly lower Phox2b immunolabeling ($P < 0.0001$) compared with $Ret^{+/+}$ GGs. (*E*) Immunostaining was performed on $Ret^{+/+}$ and $Ret^{-/-}$ GGs for the somatosensory transcription factor Brn3a and BDNF receptor TrkB. (*E*) No differences were observed in TrkB expression ($P = 0.1161$; $n = 7$ $Ret^{+/+}$ and $n = 6$ $Ret^{-/-}$ mice). (*F*) No differences were observed in Brn3a expression ($P = 0.7587$; $n = 7$ $Ret^{+/+}$ and $n = 6$ $Ret^{-/-}$ mice). (*G*) Representative immunolabeling for TuJ1 (green), Brn3a (red), and TrkB (blue). The merged image demonstrates that TrkB is widely expressed throughout the ganglion, while Brn3a expression is expressed in a polarized manner. Error bars indicate mean ± SEM; $^{**}P < 0.01$. Statistical significance for each comparison was determined with a two-tailed *t* test. (Scale bars, 100 μm.)

from E9.5 to E12.5 again had no change in total neuron numbers ($Ret^{fx/+}$: 710.25 ± 20.67 vs. $Ret^{fx/-}$: 659.60 ± 26.30; $P = 0.2056$; Fig. 3 *C* and *D*) but displayed a 29.9% reduction in the proportion of Phox2b+ neurons ($Ret^{fx/+}$: 65.92 ± 4.54% vs. $Ret^{fx/-}$: 46.24 ± 2.74%; $P = 0.0041$; Fig. 3 *C* and *D*). This was in contrast to the cohort of mice administered TMX from E14.5 to E17.5, in which no changes were observed in total neuron numbers ($Ret^{fx/+}$: 698.44 ± 35.74 vs. $Ret^{fx/-}$: 676.18 ± 23.46; $P = 0.6167$; Fig. 3*E*) or in the proportion of Phox2b+ neurons ($Ret^{fx/+}$: 63.78 ± 3.70% vs. $Ret^{fx/-}$: 61.56 ± 2.01%; $P = 0.6118$; Fig. 3*F*).

These data indicate that Ret is required for the early amplification of Phox2b expression in chemosensory neurons but is dispensable for its maintenance, concordant with the observed spatiotemporal expression pattern of Ret. Additionally, the data demonstrate that an early disruption of Ret signaling, between E9.5 and E12.5, is sufficient to irreversibly impair Phox2b expression. Lastly, Ret is not required for the survival of GG neurons, and appears to specifically regulate chemosensory cell fate determination.

Loss of Ret Results in Fungiform Papilla Chemosensory Innervation Deficits. Germ-line $Phox2b^{LacZ/LacZ}$ knockout mice have normal total GG neuron numbers (16). In these mice, however, chemosensory neurons transitioned to a molecular profile consistent with a somatosensory neuronal fate (Brn3a+, Runx1+, Drg11+), accompanied by a conversion to somatosensory axonal projection patterns. Although loss of Ret only leads to a partial disruption in Phox2b expression in chemosensory neurons, we hypothesized that chemosensory innervation of fungiform papillae would also be disrupted. Anterior tongues were collected from E18.5 $Ret^{+/+}$ and $Ret^{-/-}$ mice, and stained for TuJ1, P2X3 (a selective marker of chemosensory nerve fibers) (27), and K8 (to label early taste buds). When analyzing the entire papilla, no difference was observed in the amount of K8+ immunolabeling (Fig. 4 *A* and *B*; $P = 0.5367$) or in the density of TuJ1+ immunolabeling (Fig. 4*A*; $P = 0.3629$) between $Ret^{+/+}$ and $Ret^{-/-}$ mice. Interestingly, we observed a highly significant reduction in P2X3-labeled nerve fibers within the total fungiform papilla area (Fig. 4 *A* and *C*; 29.0% reduction; $P < 0.0001$). Correspondingly, we observed a substantial reduction in P2X3-labeled fibers when restricting analysis to the K8+ taste bud region (Fig. 4*D*; 38.9% reduction; $P < 0.0001$), despite a small but significant increase in total TuJ1+ immunolabeling within the taste bud area ($P = 0.0199$). Collectively, these data indicate that loss of Ret leads to subsequent loss of chemosensory differentiation, ultimately leading to deficits in the axon terminal expression of the neurotransmitter receptor P2X3.

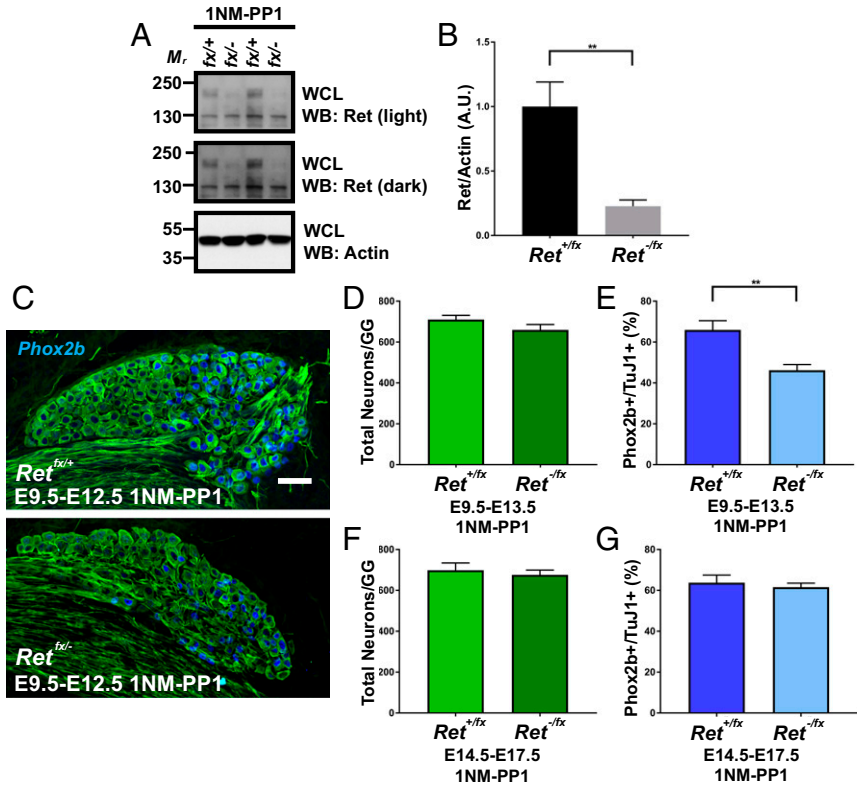

Fig. 3. Ret is required for the amplification of Phox2b early in development. (*A*) The selective Ret inhibitor 1NM-PP1 was administered to mice of the indicated genotypes at E14.5 until E18.5. Spinal cords were collected, homogenized, and detergent-extracted, followed by immunoblotting for Ret or actin (as a loading control). WB, Western blotting; WCL, whole-cell lysate. (*B*) Quantification of total Ret levels (normalized to actin). We observed a reduction of ∼77% of total Ret levels following 1NM-PP1 administration in $Ret^{fx/-}$ mice ($n = 7$) compared with $Ret^{fx/+}$ mice ($n = 10$) ($P = 0.0048$). (*C*) $Ret^{fx/+}$ and $Ret^{fx/-}$ mice were administered 1NM-PP1 daily from E9.5 to E12.5. Mice were euthanized on E13.5 and GGs were immunostained for TuJ1 and Phox2b. Similar to the results observed in Ret germ-line knockout mice, $Ret^{fx/-}$ mice had substantially fewer Phox2b+ neurons with no apparent change in total neuron number. (*D* and *E*) Total neurons (*D*) and the proportion of Phox2b+ neurons (*E*) were quantified. No difference was observed in total neuron numbers ($P = 0.2056$; $n = 4$ to 6). $Ret^{fx/-}$ had a reduction in the proportion of Phox2b+ neurons compared with $Ret^{fx/+}$ ($P = 0.0041$; $n = 4$ to 6). (*F* and *G*) $Ret^{fx/+}$ and $Ret^{fx/-}$ mice were administered 1NM-PP1 as described in *C* from E14.5 to E17.5. GGs were again immunostained for TuJ1 and Phox2b. No significant differences were observed between genotypes in the total number of neurons ($P = 0.6167$; $n = 5$ for each) (*F*) or the proportion of Phox2b+ neurons (0.6118; $n = 5$ for each) (*G*). Error bars indicate mean ± SEM; $^{**}P < 0.01$. (Scale bar, 100 μm.)

Ret Reemerges in a Unique Subpopulation of Chemosensory Neurons Postnatally. Building on the demonstrated embryonic role for GDNF-Ret signaling in prenatal chemosensory cell fate determination, we determined whether Ret expression remains extinguished postnatally. Using *Rosa26*$^{LSL\text{-}TdTomato}$; *Ret*-Cre/ER^{T2} mice, we examined Ret expression within the first week of postnatal life, a time during which the peripheral taste system is still maturing, and in adulthood, when complete maturation is reached. TMX was administered daily to P3 to P7 or P60 to P64 mice, with analysis commencing 1 d following the last TMX administration (P8 and P65, respectively). Surprisingly, given that Ret expression was nearly completely lost by late embryonic development (E18.5 time point from Fig. 1*B* regraphed in Fig. 5*C*), we observed an up-regulation of Ret within a subpopulation of chemosensory GG neurons at P8 (14.53 ± 0.64%; Fig. 5 *A*–*C*), which was further increased by P65 (20.11 ± 2.72%; Fig. 5 *B* and *C*).

The low abundance of Ret+ chemosensory GG neurons is reminiscent of subpopulations within the DRG and TG, where distinct subpopulations of neurons can be defined by their expression of neurotrophic factor receptors, somal diameter, and molecular properties, all of which influence their sensory properties (1). Within the GG chemosensory population, there is evidence that these neurons are heterogeneous in terms of size, electrical properties, and neurochemical signature (5–7, 28–31). To further characterize the Ret+ population within the GG and determine whether these neurons represent a distinct subpopulation, we analyzed the somal diameter of Ret+ chemosensory neurons (RFP+/Phox2b+) compared with Ret+ somatosensory neurons (RFP+/Phox2b−), which represent 82.28 and 17.72% of the total Ret+ neurons in the GG, respectively (Fig. S5*A*). The Ret+ chemosensory neurons, on average, were significantly larger than Ret+/Phox2b− neurons (Fig. S5 *B* and *C*; 22.34 ± 0.23 vs. 20.51 ± 0.43 μm; $P = 0.0005$), and 23.22% of Ret+ chemosensory GG neurons had somal diameters greater than 27 μm, compared with 10.53% of Ret+ somatosensory neurons. Interestingly, 66.59% of neurons expressed Ret but not TrkB (Ret+/TrkB−), whereas 33.41% of neurons expressed both receptors (Ret+/TrkB+; Fig. S5 *D* and *E*, yellow arrowheads). The Ret+/TrkB− neurons were typically larger than Ret+/TrkB+ neurons ($P < 0.0058$; 23.81 ± 0.26 μm for Ret+/TrkB− compared with 22.65 ± 0.33 μm for Ret+/TrkB+) and also Ret−/TrkB+ neurons ($P = 0.0001$; 19.28 ± 0.15 μm for Ret−/TrkB+). Ret+/TrkB+ neurons were also significantly larger than the Ret−/TrkB+ neurons ($P < 0.0001$). These data argue for the existence of at least three distinct subpopulations of neurons within the GG based on morphological properties of the cells as well as neurotrophic factor receptor expression.

Ret signaling defines a subpopulation of large-diameter neurofilament heavy chain-enriched (NF200+) low-threshold mechanoreceptors within the DRG (13, 32). Given that GG Ret+ neurons were of larger diameter, we examined whether Ret+ GG neurons expressed NF200. Additionally, we analyzed which GFRα coreceptors were expressed within GG neurons. Interestingly, we observed GFRα1 immunoreactivity within Ret+/NF200+ GG neurons (Fig. 5*D*) but were unable to detect either GFRα2+ or GFRα3+ GG neurons (Fig. S6*A*), despite the presence of strong immunoreactivity for both coreceptors within the TG (Fig. S6*B*), as has been previously reported (33, 34). Additionally, to further characterize the NF200+ population of neurons, we analyzed adult *Rosa26*$^{LSL\text{-}TdTomato/+}$; *Phox2b-Cre*$^{tg/+}$ GGs. As expected, Brn3a and Phox2b immunolabelings were almost mutually exclusive, with only rare examples of double-labeled neurons (green arrowheads). Although examples of Brn3a/NF200+ neurons (yellow arrowheads) were observed, Phox2b/NF200+ neurons (blue arrows) were much more abundant, indicating that a large population of transcriptionally chemosensory neurons expresses the mechanoreceptor marker NF200 (Fig. S6*C*). To validate the postnatal increase in expression, lysates were prepared from P0 or adult GG and quantitative immunoblotting was performed (Fig. S6*D*). As expected, we observed a statistically significant increase in normalized Ret expression in adult mice compared with P0 mice (Fig. S6*E*), further substantiating the

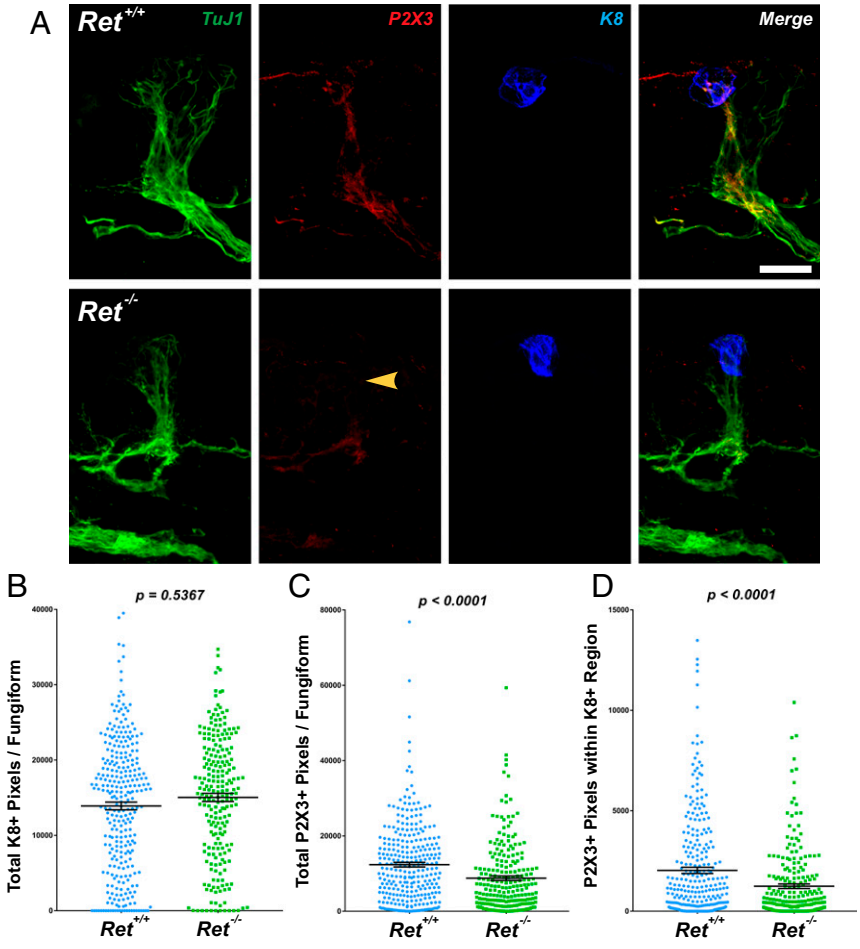

Fig. 4. Loss of Ret results in deficits in fungiform papilla chemosensory innervation. (*A*) Tongues were collected from E18.5 $Ret^{+/+}$ and $Ret^{-/-}$ mice, serially sectioned at 50 μm, and immunostained for TuJ1 (green), P2X3 (red), and K8 (blue) and merged. Many more examples of FPs lacking apically projecting P2X3+ fibers were observed in $Ret^{-/-}$ compared with $Ret^{+/+}$ tongues (yellow arrowhead). (*B*) All fungiform papillae from $n = 4$ mice were imaged ($n = 300$ $Ret^{+/+}$ FPs and $n = 230$ $Ret^{-/-}$ FPs) and quantified as described in *Experimental Procedures*. When analyzing the entire papilla, no differences were observed in the number of K8+ pixels per FP ($P = 0.5367$). (*C*) A highly significant reduction in P2X3+ pixels was observed in $Ret^{-/-}$ mice ($P < 0.0001$). (*D*) When analyzing only the nerve fibers present within the K8+ region, P2X3+ pixels were substantially reduced ($P < 0.0001$). The graphs in *B*–*D* display individual data points (colored circles and squares), while the mean ± SEM is indicated by the black lines. (Scale bar, 25 μm.)

postnatal increase. Collectively, these data indicate that Ret expression reemerges postnatally within large-diameter chemosensory neurons expressing Ret, GFRα1, and NF200 and, thus, molecularly define a unique subpopulation of lingual GG sensory neurons that are likely to be mechanoreceptors.

Examination of Ret+ Nerve Fibers Within Fungiform Papillae. To investigate whether Ret-expressing chemosensory GG neurons project into TBs, we immunostained anterior tongues dissected from TMX-labeled adult $Rosa26^{LSL\text{-}TdTomato}$; *Ret*-Cre/$ER^{T2}$ mice for TuJ1 (green), RFP (Ret; red), and K8 (blue). Fungiform papillae were imaged in their entirety, and we documented anterior, middle, and posterior locations on the tongue. To determine the projection pattern of Ret+ nerve fibers, maximum-projection images were utilized, along with the original composite z stack, to assess whether nerve fibers were terminating within the K8+ taste bud area. RFP+ nerve fibers (red) terminating within the K8+ area were classified as intragemmal, while those terminating outside the K8+ area were classified as extragemmal. There was variability in the extent of innervation of fungiform papillae (FPs), although 94.89% of all FPs had either a combination of extragemmal and intragemmal (Fig. 6*A*) Ret+ nerve fibers or exclusively extragemmal nerve fibers (Fig. 6*B*). To quantify the extent of Ret+ innervation within each category (extragemmal and intragemmal), we further divided each group into three categories: (*i*) no innervation; (*ii*) fewer than three nerve branches; and (*iii*) greater than three nerve branches. When analyzing extragemmal Ret+ fibers, we observed that 85.2% of FPs were extensively innervated by Ret+ fibers (>3 branches), 13.1% of FPs were moderately innervated by Ret+ fibers (one to three branches), and 1.7% of FPs had no extragemmal Ret+ fibers (Fig. 6*C*), although in all three of these cases no nerve fibers were observed. When analyzing intragemmal Ret+ fibers (those within the K8+ region), we observed that 13.1% of FPs had >3 branches, 31.8% had one to three branches, and 56.25% had no intragemmal Ret+ nerve fibers (Fig. 6*D*). To determine whether the location of FPs on the dorsal tongue influenced the innervation density or pattern, when normalizing for the total number of FPs counted within each region (tip vs. middle vs. posterior tongue), we observed no changes in the distribution of either extragemmal or intragemmal nerve fibers (Fig. S7 *A* and *B*). Additionally, in 7.96% of FPs, we observed elongated Ret+ taste receptor cells (TRCs) which extended the full length of the taste bud (Fig. S7*C*), and in all instances these were present on the anterior-most tip of the tongue.

Differences in the innervation patterns have been reported between extragemmal nerve fibers originating from the $Phox2b^{-}$/$Brn3a^{+}$ TG, somatosensory in nature, and intragemmal nerve fibers originating from the $Phox2b^{+}$/$Brn3a^{-}$ GG, chemosensory in nature (18, 35). We further examined this model using adult $Rosa26^{LSL\text{-}TdTomato/+}$; $Phox2b\text{-}Cre^{tg/+}$ mice to selectively label and trace GG/CT chemosensory afferent fibers within FPs. To our surprise, when analyzing FPs, we observed that 31.8% of FPs analyzed had >3 nerve fibers outside the K8+ region (Fig. S8*A*), 18.5% of FPs had one to three nerve fibers outside the K8+ region (Fig. S8*B*), and 49.7% of FPs had no extragemmal nerve fibers (Fig. S8*C*) (quantifications provided in Fig. S8*D*). Confirming previous studies, all papillae analyzed (151/151) had intragemmal labeling. These data suggest that some Phox2b+ GG neurons may project extragemmally, to an area adjacent to

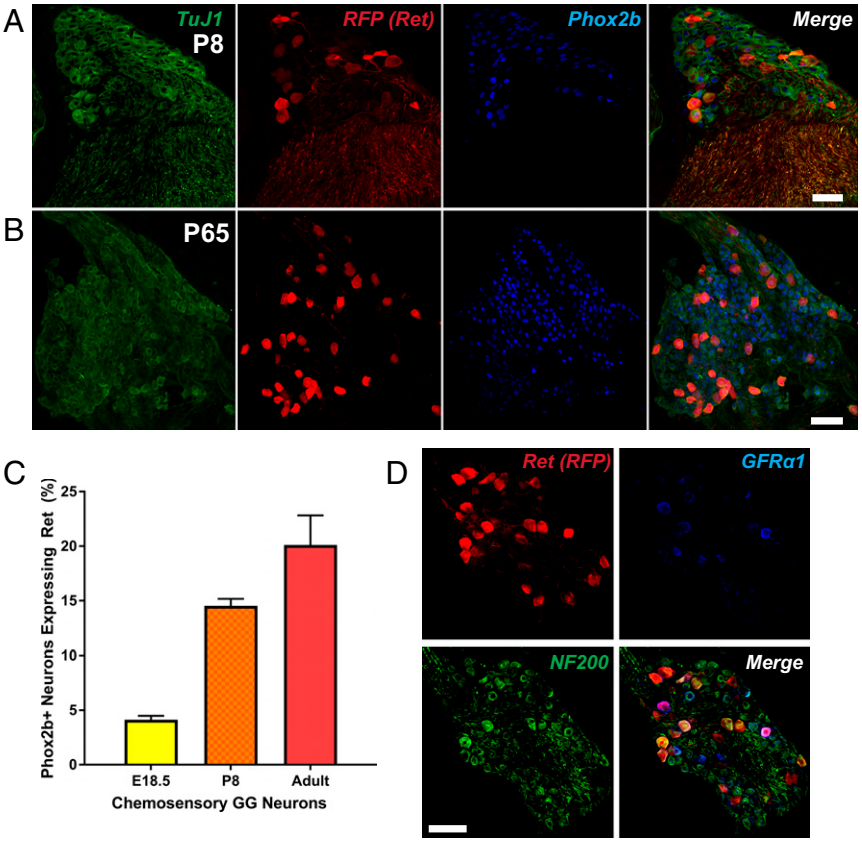

Fig. 5. Ret is expressed postnatally in a subpopulation of GFRα1/NF200+ chemosensory neurons. (*A* and *B*) Ret-Cre/ER^{T2}; *Rosa26*$^{LSL\text{-}TdTomato/+}$ mice were administered TMX at P3 to P7 and analyzed at P8 (*A*) or P60 to P64 and analyzed at P65 (*B*). GGs were stained for TuJ1 (green), RFP (indicating Ret; red), and Phox2b (blue). (*C*) Quantification of Ret expression at E18.5 (regraphed from Fig. 1*B*), P8, and P65 indicated that a substantial number of chemosensory neurons up-regulate Ret postnatally. (*D*) Adult GGs from TMX-labeled Ret-Cre/ER^{T2}; *Rosa26*$^{LSL\text{-}TdTomato/+}$ were immunostained for RFP (red), GFRα1 (blue), and mechanoreceptor marker neurofilament heavy chain NF200. Many neurons demonstrated overlapping expression of Ret, GFRα1, and NF200 (representative images from $n = 4$ individual experiments). Error bars indicate mean ± SEM. (Scale bars, 50 μm.)

the K8+ taste bud region. Thus, while analysis of intragemmal nerve fibers is a strong predictor of chemosensory innervation origin, analysis of extragemmal innervation may represent a mixture of somatosensory TG afferents and Phox2b+/chemosensory GG/CT afferents. However, we cannot rule out the potential contribution of Phox2b+ sympathetic nerve fibers to the FPs. Although only 43.75% of Ret+ nerve fibers project intragemmally, a proportion of the observed extragemmal nerve fiber labeling (98.30% of all FPs) may also be of chemosensory origin.

GDNF Is Expressed Within Fungiform Papillae but Not Geniculate Ganglion Neurons. Based on the expression of GFRα1 within GG neurons and the complete lack of GFRα2 and GFRα3, the expression pattern of GDNF was examined. We used *Rosa26*$^{LSL\text{-}TdTomato}$; *GDNF*-IRES-Cre/ER^{T2} mice. Adult mice were administered TMX on 5 successive days and euthanized, and GG and anterior tongues were collected. Tongues were immunostained for TuJ1, RFP (GDNF), and K8 or E-cadherin (E-Cad), a marker of cells within the lingual epithelium. Importantly, GDNF was expressed predominantly within the basal epithelium layer, both in the fungiform papilla walls as well as the cells within and around the taste bud (Fig. 6*E*). No GDNF+ nerve fibers were observed, indicating a lack of GDNF expression by GG neurons themselves. Correspondingly, analysis of the GG confirmed this result, as no examples of GDNF+ neurons were observed within the GG (Fig. S8*E*), although GDNF+ satellite cells within the facial nerve were occasionally seen.

Ablation of Ret+ Geniculate Neurons Results in a Loss of Tactile but Not Chemical or Cold Responses. We next sought to determine whether Ret+ GG neurons underlie a particular lingual sensory modality. *Ret*-Cre/ER^{T2} mice were crossed with a transgenic *Rosa26*$^{LSL\text{-}DTA/LSL\text{-}DTA}$ line (abbreviated *DTA*$^{+/+}$), whereupon TMX administration leads to ablation of all Ret+ cells, thereby eliminating all GG neurons expressing Ret (Fig. S9*A*). These DTA mice have been previously characterized, and show very rapid loss of cells following Cre induction (36). TMX was administered to adult *Ret*$^{Cre/+}$; *DTA*$^{+/+}$ (Ret-ablated) mice or *Ret*$^{+/+}$; *DTA*$^{+/+}$ (wild-type) mice, as a control, for 3 d, followed by whole-nerve recording from the CT nerve. In all mice, efficacy of Ret+ neuron ablation was confirmed histologically following electrophysiological recordings by analyzing total Phox2b+ neurons. Ret-ablated mice had fewer Phox2b+ neurons compared with WT mice (WT: 384.5 ± 15.6 neurons vs. Ret-ablated: 336.6 ± 27.8 neurons; 12.5% reduction; $n = 9$ and $n = 14$, respectively; representative images are shown in Fig. S9*B*), although some variability was observed. Given our data indicating that ∼20% of adult neurons express Ret (Fig. 5*A*) and most of these (82.28%) neurons are chemosensory, we reasoned that our ablation efficacy was similar to the expected value (16.5%). Additionally, other phenotypic effects in Ret-ablated mice were observed that indicated a reliable ablation of Ret+ cells, such as an enlarged gastrointestinal tract, indicative of a Hirschsprung's-like phenotype. Interestingly, when focusing our analysis on the mice verified to have strong deletion meeting the inclusion criteria (*Experimental Procedures*), we observed no differences in chemical responses (Fig. 7*A* and Fig. S9*C*) or cold responses (Fig. 7*B* and Fig. S9*D*) in any of the Ret-ablated mice compared with WT controls. In stark contrast, we observed a complete loss of tactile responses in 4/7 Ret-ablated mice, despite the presence of spontaneous nerve activity. Additionally, we observed a substantially weakened tactile response in 1/7 Ret-ablated mouse, and no change in tactile responses in two Ret-ablated mice (Fig. 7*C* and Fig. S9*E*). Because responses to tactile stimuli are rapidly adapting and not sustained, we present raw responses rather than summated recordings for tactile stimulation. These data indicate that the Ret-expressing GG neurons projecting via the chorda tympani nerve to FPs are a population of functionally

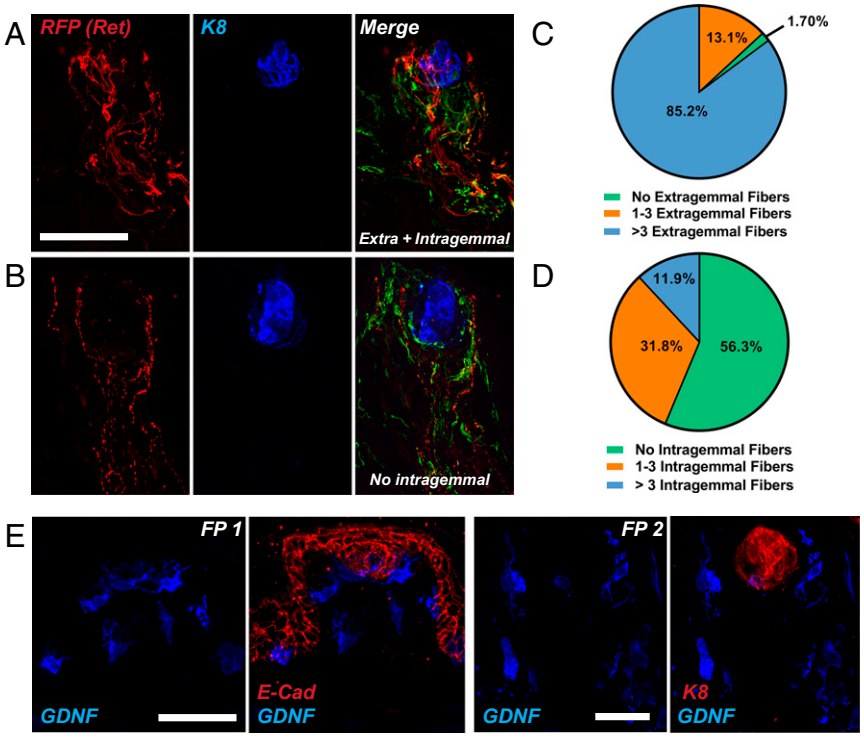

Fig. 6. Distribution pattern of Ret+ nerve fibers and GDNF+ cells within fungiform papillae. (*A*) Whole tongues from adult *Ret*-Cre/ER^{T2}; *Rosa26*$^{LSL\text{-}TdTomato/+}$ mice were immunostained for RFP (indicates Ret; red), K8 (blue), and TuJ1 (green; present in merged image). One hundred seventy-six FPs from $n = 5$ individual mice were imaged and the pattern of Ret expression was categorized as intragemmal (within the K8+ region) or extragemmal (outside the K8+ region). This is an example of an FP with extensive (>3 fibers) intragemmal and extragemmal innervation by Ret+ fibers. (*B*) Example of an FP with extensive (>3 fibers) extragemmal labeling but no intragemmal Ret+ fibers. (*C*) Quantification of the innervation density of Ret+ extragemmal fibers indicates that the vast majority of FPs have extragemmal fibers present (98.3%), most of which (85.2%) have greater than three fibers. (*D*) Quantification of the innervation density of intragemmal Ret+ fibers demonstrates that many FPs (43.7%) have an intragemmal projection pattern. (*E*) Five daily doses of TMX were administered to adult *GDNF*-IRES-Cre/ER^{T2}; *Rosa26*$^{LSL\text{-}TdTomato/+}$ via i.p. injection. Tongues were then fixed, preserved, serially sectioned, and immunostained for RFP (indicating GDNF; blue) and E-cadherin (red; *Left*, FP 1) or K8 (red; *Right*, FP 2). All FPs were imaged from $n = 4$ individual mice. We observed a variable pattern of expression of GDNF within the TB region (ranging from 0 to 2 cells generally present within the basal aspect of the TB) but strong labeling of GDNF in the perigemmal space immediately surrounding the TB. In addition, GDNF+ cells were observed in the E-Cad+ trenches at the base of the FP. On occasion, GDNF+ cells were observed in the mesenchymal core of the FP. (Scale bars, 50 μm.) In all cases, Cre-negative littermate controls were always utilized to control for RFP immunostaining specificity.

unique mechanoreceptors, although we cannot rule out that they are multimodal in function.

Discussion

Ret Specifies Chemosensory Cell Fate Acquisition. The coexistence of distinct chemosensory and somatosensory neurons within the same ganglion, each with unique transcriptional codes and subsequent peripheral and central projection patterns, makes the GG an interesting model in which to study sensory neuron specification. Our analysis of mice with germ-line Ret deletion (Fig. 2 *A*–*C*), conditional deletion of Ret following Phox2b expression (Fig. S4), and temporal pharmacologic inhibition of Ret (Fig. 3 *C*–*G*) supports the notion that Ret is required for Phox2b amplification but not its initiation or maintenance. Interestingly, Ret deletion did not impact neuronal survival, and we observed no significant change in the expression pattern of the neurotrophic

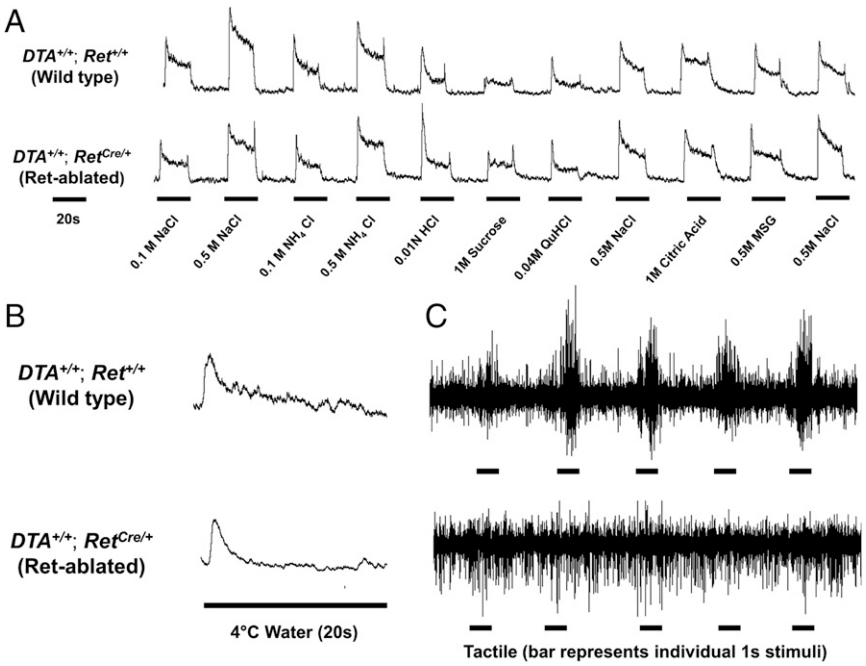

Fig. 7. Ablation of Ret+ neurons results in deficits in tactile but not chemical or thermal responses. (*A* and *B*) Chorda tympani integrated nerve responses to taste stimuli (*A*) and cold stimuli (*B*) are unaffected in *Ret*$^{Cre/+}$; *DTA*$^{+/+}$ mice (Ret-ablated; *Lower*) compared with control animals. (*C*) A representative trace demonstrating the loss of chorda tympani responses to tactile stimulation (*Upper*, WT; *Lower*, Ret-ablated). Of the seven *Ret*$^{Cre/+}$; *DTA*$^{+/+}$ mice tested, four had loss of tactile responses, one had substantially weakened responses, and two had a residual response (additional traces are displayed in Fig. S9). Despite the loss of tactile responses, spontaneous neural activity remains intact in Ret-ablated nerves. Because responses to tactile stimuli are not sustained, tactile responses are not integrated but presented as whole-nerve recordings.

factor receptor TrkB (Fig. 2 *D* and *F*), the neurotrophic signaling pathway supporting GG neurons during axon guidance and target-dependent survival (10). Additionally, the loss of Ret impaired chemosensory innervation of developing taste buds within the fungiform papillae (Fig. 4), arguing that loss of chemosensory cell fate leads to a subsequent impairment in peripheral projections of GG neurons. However, whether this reflects a complete loss of these nerve fibers, or simply a loss of the chemosensory-specific neurotransmitter receptor P2X3 used to label these fibers, is unknown.

A previous study analyzing $Phox2b^{LacZ/LacZ}$ knockout mice demonstrated that loss of Phox2b in chemosensory GG neurons results in acquisition of Brn3a expression (16). Despite loss of Phox2b expression, we did not see an increase in the proportion of the somatosensory neurons expressing the determinant Brn3a (Fig. 2 *D* and *E*). Although our data support the notion that Ret promotes Phox2b expression within chemosensory neurons, and its removal results in a substantial loss of Phox2b, Ret deletion is not synonymous with the complete knockout of Phox2b. These results may reflect the partial nature of the Ret knockout phenotype, as only a 30 to 40% reduction in the proportion of chemosensory neurons expressing Phox2b was observed (depending on the experimental model analyzed), with many more neurons having a qualitative reduction in Phox2b expression, and some residual expression remaining. Two previous studies investigating the interrelationship of Brn3a with Ret in the DRG (37) and the TG (38) demonstrated that Brn3a and Ret are spatially segregated in their expression patterns, and that Ret+ neurons are spared in Brn3a knockout mice. For these reasons, it is perhaps not surprising that Ret deletion does not impact Brn3a. Likely, the residual low level of Phox2b expression is sufficient to inhibit Brn3a expression within these neurons, suggesting that the role of Ret in this process is to amplify the expression of Phox2b but that Ret signaling itself does not directly influence Brn3a expression. Building on the aforementioned studies and based on our results, we propose a model in which (*i*) Phox2b induces Ret expression in chemosensory neurons; (*ii*) Ret, acting as part of a positive feedback loop, amplifies the expression of Phox2b during the early embryonic window before target innervation; and (*iii*) Phox2b represses Brn3a expression. Thus, there is a critical window in which the interaction between Ret and Phox2b is required for the acquisition of the appropriate transcriptional fate.

Ret Specifies a Distinct Subpopulation of Chemosensory Neurons Postnatally. Based on experiments analyzing Ret reporter mice, ∼20% of GG neurons express Ret in adulthood. These findings bear some similarity to other sensory neuron populations wherein subpopulations of neurons with differential neurotrophic factor receptor expression can be delineated based on molecular, physical, and functional characteristics (2). Most Ret+ GG neurons were chemosensory as defined by Phox2b expression (82.28%; Fig. S3*A*), with approximately a 2:1 ratio of neurons lacking TrkB (Ret+/TrkB−) compared with neurons expressing both receptors (Ret+/TrkB+) (Fig. S5 *D* and *E*). These neurons were large in diameter, compared with neurons positive for only TrkB (Fig. S5 *F* and *G*), and expressed the mechanoreceptor marker NF200 (Fig. 5*D*). Additionally, when analyzing GFRα coreceptors present within the GG, which are required for downstream Ret signaling, only GFRα1 was detectable (Fig. 5*D* and Fig. S6 *A* and *B*). Correspondingly, we observed many Ret+ nerve fibers, both intragemmal and extragemmal in nature (Fig. 6 *A*–*D*), as well as many GDNF+ cells within the fungiform papillae, including those within and immediately surrounding the taste bud region (Fig. 6*E*). Finally, electrophysiological recordings of mice in which Ret+ neurons were ablated indicate that these Ret+ neurons function as a unique subpopulation of GG/CT afferent mechanoreceptive neurons (Fig. 7).

While several studies have begun to expand our knowledge of the heterogeneity within the GG (5–7, 30, 39, 40), our understanding of the cellular basis defining the multimodality of orofacial chemosensory neurons remains quite rudimentary in comparison with TG and DRG somatosensory neurons, where as many as 11 molecularly distinct subpopulations have been described (41). This study demonstrates the existence of a molecularly, morphologically, and functionally distinct lingual GG neuron subtype. Given that Ret+ neurons are chemosensory (Phox2b+) in molecular profile but have physiological and morphological properties of mechanoreceptors, they represent a unique population dissimilar from pinna-projecting somatosensory neurons within the GG, lingually projecting chemosensory neurons within the GG, as well as Ret+ mechanoreceptors described in the TG and DRG. As such, the specific nomenclature for these transcriptionally chemosensory but functionally somatosensory neurons is a subject for debate. Interestingly, mice administered pharmacologic purinergic receptor inhibitors (42) as well as P2X2/P2X3 double-knockout mice (39) lose chemical but not tactile responses. Furthermore, loss of the fungiform TBs following pharmacologic inhibition of the sonic hedgehog pathway disrupts chemical but not tactile chorda tympani responses (40), suggesting that the taste bud itself is not required for the mechanical responses. Thus, it remains unknown what the gating mechanisms are for these mechanical responses, as well as what presynaptic lingual sensory end organs are responsible for communicating with these fibers. Further defining the receptive fields and adaptation properties of these neurons remains an important future direction, as does the identification of the physiological significance of these neurons.

Experimental Procedures

Animals. All experiments were carried out in compliance with the guidelines of the Association for Assessment and Accreditation of Laboratory Animal Care International and approved by the Institutional Animal Care and Use Committee of the University of Michigan.

Production of Embryos, Tamoxifen Delivery, and 1NM-PP1 Administration. $Ret^{fx/fx}$ (14), $Ret^{-/-}$ (22), *Ret*-Cre/ER^{T2} (13), $Rosa26^{LSL\text{-}TdTomato/+}$ (43), *Phox2b*-Cre$^{tg/+}$ (44), *GDNF*-IRES-Cre/ER^{T2} (21), and $Rosa26^{LSL\text{-}DTA}$ (36) mice have all been previously described. All mice were maintained in mixed genetic backgrounds and all comparisons were made using littermates. For timed mating experiments, noon of the day on which a vaginal plug was detected was considered E0.5. For the experiments tracing Ret or GDNF expression, tamoxifen (T5648; Sigma-Aldrich) was dissolved in corn oil and administered via i.p. injection at a dose of 0.25 mg/g body weight, at time points described in the figure legends, with Cre-negative littermate controls analyzed in all experiments. For the experiments utilizing the pharmacologic inhibitor 1NM-PP1 (529581; EMD Millipore), pregnant dams were given i.p. injections daily (16.6 ng/g body weight, as previously described) (25) at the indicated time points, and 1NM-PP1 was also maintained in the drinking water at a concentration of 1 mM to maintain chemical inhibition. Detailed descriptions of fixation, sectioning, immunostaining, tissue lysis, and quantitative immunoblotting procedures can be found in *Supporting Information*.

Neuron Counts, Somal Diameter Measurements, and Innervation Classification. The average somal diameter of GG neurons was observed to be 22.02 ± 0.20 μm, and for this reason we performed cell counts on 20-μm serial sections of the entire GG. For experiments analyzing TGs from $Rosa26^{LSL\text{-}TdTomato/+}$; *Phox2b-Cre*$^{tg/+}$ mice, counts were performed on three sections per ganglion, ∼200 μm apart. Somal diameters were measured at the widest aspect of each neuron using the TuJ1 channel. For innervation classifications, maximum projections as well as the original composite *z*-stack images were utilized to assess whether nerve fibers were terminating within the K8+ taste bud area. Nerve fibers terminating within the K8+ area were classified as intragemmal, while those terminating outside the K8+ area were classified as extragemmal. Greater than three nerve fibers was chosen as an arbitrary cutoff point to subcategorize FPs into those having extensive (>3 fibers) or slight to moderate (one to three fibers) innervation density. Detailed description of the protocol used for Fiji quantification of fungiform papilla innervation and Phox2b expression is expanded in *Supporting Information*.

Statistics and Data Analysis. All results are expressed as the mean ± SEM. All statistical tests were performed using two-tailed parameters with a significance level of $P \leq 0.05$ to test for statistical significance. A two-tailed Student's *t* test was utilized for all comparisons between two treatment groups. Comparisons between more than two treatment groups were performed with one-way ANOVA. The data were originally entered into Excel and imported into GraphPad Prism, which was used for all statistical tests and graph production. The presence of asterisks indicates statistical significance: $*P < 0.05$, $**P < 0.01$, $***P < 0.001$, $****P < 0.0001$. Sample sizes are indicated in the results and figure legends. No sample sizes of fewer than three independent experiments were utilized. For all GG counts, when possible, each animal represents the average count of two GGs to increase statistical accuracy. For all pooled analyses of FPs, statistical tests were performed on both the pooled data and the individualized animal data to ensure that no differences in outcome were obtained.

Chorda Tympani Nerve Recordings. Mice were anesthetized with a ketamine-xylazine mixture (80 to 100 mg/kg ketamine, 5 to 10 mg/kg xylazine, delivered i.p.) and maintained with ketamine (80 to 100 mg/kg) as needed. The CT was exposed by a lateral approach, dissected, cut centrally, and placed on a recording electrode. An indifferent electrode was placed in nearby tissue. Amplified neural activity was observed in an oscilloscope, passed through an analog-to-digital converter, and recorded using the Spike2 program (Cambridge Electronic Design). The amplified signal was also passed through an integrator circuit with a 0.5-s time constant. Tactile stimuli consisted of stroking the anterior tongue quadrant five times over a period of 5 s, while thermal stimuli consisted of application of 4 °C water. The indicated chemical stimuli were dissolved in distilled water at room temperature, and 3 to 5 mL was applied to the tongue using a syringe. Chemicals remained on the tongue for 20 s, followed by a distilled water rinse for 30 s. NaCl and NH_4Cl were applied throughout the nerve recording to monitor stability and changes from baseline. The initial increase in integrated recordings at onset and rinse of chemicals from the tongue includes the stimulus artifact, seen when a chemical or rinse contacts the tongue (7), and the initial high-frequency transient response can be useful for measuring response latency or assessing temporal aspects of the summated response. Neither integrated onset nor offset is related to the somatosensory response. The tactile responses observed were to a moving, light stroking stimulus only.

ACKNOWLEDGMENTS. We thank Dr. Archana Kumari, Alan Halim, Esther Suh, and Tommy Vu for technical assistance. We thank Dr. Wenqin Liu and Dr. Hideki Enomoto for providing *Ret*-Cre/ER^{T2} mice, and Dr. David Ginty and Dr. Joseph Savitt for providing *Ret*$^{fx/fx}$ mice. We thank Robin Krimm for providing *TrkB*$^{GFP/GFP}$ tissues and for technical expertise. Support was provided (to C.R.D.) through National Institute of Dental and Craniofacial Research Grant T32 DE007057 and Fellowship F30 DE023479. These experiments were supported by National Institute of Neurological Disorders and Stroke Grant R01 NS089585 and National Institute on Deafness and Other Communication Disorders Grants R01 DC015799 (to B.A.P.) and R01 DC014428 (to C.M.M. and R.M.B.).

1. Liu Y, Ma Q (2011) Generation of somatic sensory neuron diversity and implications on sensory coding. *Curr Opin Neurobiol* 21:52–60.
2. Lallemend F, Ernfors P (2012) Molecular interactions underlying the specification of sensory neurons. *Trends Neurosci* 35:373–381.
3. Li L, et al. (2011) The functional organization of cutaneous low-threshold mechanosensory neurons. *Cell* 147:1615–1627.
4. Chen CL, et al. (2006) Runx1 determines nociceptive sensory neuron phenotype and is required for thermal and neuropathic pain. *Neuron* 49:365–377.
5. Boudreau JC, Bradley BE, Bierer PR, Kruger S, Tsuchitani C (1971) Single unit recordings from the geniculate ganglion of the facial nerve of the cat. *Exp Brain Res* 13:461–488.
6. Lundy RF, Jr, Contreras RJ (1999) Gustatory neuron types in rat geniculate ganglion. *J Neurophysiol* 82:2970–2988.
7. Yokota Y, Bradley RM (2016) Receptive field size, chemical and thermal responses, and fiber conduction velocity of rat chorda tympani geniculate ganglion neurons. *J Neurophysiol* 115:3062–3072.
8. Krimm RF (2007) Factors that regulate embryonic gustatory development. *BMC Neurosci* 8(Suppl 3):S4.
9. Patel AV, Krimm RF (2012) Neurotrophin-4 regulates the survival of gustatory neurons earlier in development using a different mechanism than brain-derived neurotrophic factor. *Dev Biol* 365:50–60.
10. Ma L, Lopez GF, Krimm RF (2009) Epithelial-derived brain-derived neurotrophic factor is required for gustatory neuron targeting during a critical developmental period. *J Neurosci* 29:3354–3364.
11. Meng L, Huang T, Sun C, Hill DL, Krimm R (2017) BDNF is required for taste axon regeneration following unilateral chorda tympani nerve section. *Exp Neurol* 293:27–42.
12. Enomoto H, et al. (2001) RET signaling is essential for migration, axonal growth and axon guidance of developing sympathetic neurons. *Development* 128:3963–3974.
13. Luo W, Enomoto H, Rice FL, Milbrandt J, Ginty DD (2009) Molecular identification of rapidly adapting mechanoreceptors and their developmental dependence on Ret signaling. *Neuron* 64:841–856.
14. Luo W, et al. (2007) A hierarchical NGF signaling cascade controls Ret-dependent and Ret-independent events during development of nonpeptidergic DRG neurons. *Neuron* 54:739–754.
15. Airaksinen MS, Saarma M (2002) The GDNF family: Signalling, biological functions and therapeutic value. *Nat Rev Neurosci* 3:383–394.
16. D'Autréaux F, Coppola E, Hirsch M-R, Birchmeier C, Brunet J-F (2011) Homeoprotein Phox2b commands a somatic-to-visceral switch in cranial sensory pathways. *Proc Natl Acad Sci USA* 108:20018–20023.
17. Rochlin MW, O'Connor R, Giger RJ, Verhaagen J, Farbman AI (2000) Comparison of neurotrophin and repellent sensitivities of early embryonic geniculate and trigeminal axons. *J Comp Neurol* 422:579–593.
18. Dauger S, et al. (2003) Phox2b controls the development of peripheral chemoreceptors and afferent visceral pathways. *Development* 130:6635–6642.
19. Fode C, et al. (1998) The bHLH protein NEUROGENIN 2 is a determination factor for epibranchial placode-derived sensory neurons. *Neuron* 20:483–494.
20. Mistretta CM, Liu HX (2006) Development of fungiform papillae: Patterned lingual gustatory organs. *Arch Histol Cytol* 69:199–208.
21. Cebrian C, Asai N, D'Agati V, Costantini F (2014) The number of fetal nephron progenitor cells limits ureteric branching and adult nephron endowment. *Cell Rep* 7:127–137.
22. Schuchardt A, D'Agati V, Larsson-Blomberg L, Costantini F, Pachnis V (1994) Defects in the kidney and enteric nervous system of mice lacking the tyrosine kinase receptor Ret. *Nature* 367:380–383.
23. Huang EJ, et al. (2001) Brn3a is a transcriptional regulator of soma size, target field innervation and axon pathfinding of inner ear sensory neurons. *Development* 128:2421–2432.
24. Patel AV, Krimm RF (2010) BDNF is required for the survival of differentiated geniculate ganglion neurons. *Dev Biol* 340:419–429.
25. Chen X, et al. (2005) A chemical-genetic approach to studying neurotrophin signaling. *Neuron* 46:13–21.
26. Tsui-Pierchala BA, Milbrandt J, Johnson EM, Jr (2002) NGF utilizes c-Ret via a novel GFL-independent, inter-RTK signaling mechanism to maintain the trophic status of mature sympathetic neurons. *Neuron* 33:261–273.
27. Ishida Y, et al. (2009) P2X(2)- and P2X(3)-positive fibers in fungiform papillae originate from the chorda tympani but not the trigeminal nerve in rats and mice. *J Comp Neurol* 514:131–144.
28. Kitamura K, Kimura RS, Schuknecht HF (1982) The ultrastructure of the geniculate ganglion. *Acta Otolaryngol* 93:175–186.
29. Grigaliunas A, Bradley RM, MacCallum DK, Mistretta CM (2002) Distinctive neurophysiological properties of embryonic trigeminal and geniculate neurons in culture. *J Neurophysiol* 88:2058–2074.
30. Fei D, Krimm RF (2013) Taste neurons consist of both a large TrkB-receptor-dependent and a small TrkB-receptor-independent subpopulation. *PLoS One* 8:e83460.
31. Al-Hadlaq SM, Bradley RM, MacCallum DK, Mistretta CM (2003) Embryonic geniculate ganglion neurons in culture have neurotrophin-specific electrophysiological properties. *Neuroscience* 118:145–159.
32. Bourane S, et al. (2009) Low-threshold mechanoreceptor subtypes selectively express MafA and are specified by Ret signaling. *Neuron* 64:857–870.
33. Heuckeroth RO, et al. (1999) Gene targeting reveals a critical role for neurturin in the development and maintenance of enteric, sensory, and parasympathetic neurons. *Neuron* 22:253–263.
34. Naveilhan P, et al. (1998) Expression and regulation of GFRalpha3, a glial cell line-derived neurotrophic factor family receptor. *Proc Natl Acad Sci USA* 95:1295–1300.
35. Zaidi FN, Whitehead MC (2006) Discrete innervation of murine taste buds by peripheral taste neurons. *J Neurosci* 26:8243–8253.
36. Wu S, Wu Y, Capecchi MR (2006) Motoneurons and oligodendrocytes are sequentially generated from neural stem cells but do not appear to share common lineage-restricted progenitors in vivo. *Development* 133:581–590.
37. Zou M, Li S, Klein WH, Xiang M (2012) Brn3a/Pou4f1 regulates dorsal root ganglion sensory neuron specification and axonal projection into the spinal cord. *Dev Biol* 364:114–127.
38. Huang EJ, et al. (1999) POU domain factor Brn-3a controls the differentiation and survival of trigeminal neurons by regulating Trk receptor expression. *Development* 126:2869–2882.
39. Finger TE, et al. (2005) ATP signaling is crucial for communication from taste buds to gustatory nerves. *Science* 310:1495–1499.
40. Kumari A, et al. (2015) Hedgehog pathway blockade with the cancer drug LDE225 disrupts taste organs and taste sensation. *J Neurophysiol* 113:1034–1040.
41. Usoskin D, et al. (2015) Unbiased classification of sensory neuron types by large-scale single-cell RNA sequencing. *Nat Neurosci* 18:145–153.
42. Vandenbeuch A, et al. (2015) Postsynaptic P2X3-containing receptors in gustatory nerve fibres mediate responses to all taste qualities in mice. *J Physiol* 593:1113–1125.
43. Madisen L, et al. (2010) A robust and high-throughput Cre reporting and characterization system for the whole mouse brain. *Nat Neurosci* 13:133–140.
44. Rossi J, et al. (2011) Melanocortin-4 receptors expressed by cholinergic neurons regulate energy balance and glucose homeostasis. *Cell Metab* 13:195–204.
45. Schindelin J, et al. (2012) Fiji: An open-source platform for biological-image analysis. *Nat Methods* 9:676–682.